CHEMISTRY OF MATERIALS

Article

pubs.acs.org/cm

# Inverted Surface Dipoles in Fluorinated Self-Assembled Monolayers

Oussama Zenasni, Maria D. Marquez, Andrew C. Jamison, Han Ju Lee, Arkadiusz Czader, and T. Randall Lee*

Departments of Chemistry and Chemical Engineering and the Texas Center for Superconductivity, University of Houston, Houston, Texas 77204-5003, United States

Supporting Information

**ABSTRACT:** The presence of surface dipoles in self-assembled monolayers (SAMs) gives rise to profound effects on the interfacial properties of the films. For example, $CF_3$-terminated alkanethiolate films are surprisingly more wettable toward polar contacting liquids than analogous hydrocarbon SAMs due to the fluorocarbon-to-hydrocarbon transition ($CF_3$−$CH_2$) at the interface (i.e., the presence of a strong "FC−HC" surface dipole). This report explores the converse situation by analyzing partially fluorinated monolayers (FSAMs) in which the polarity of the surface dipole has been inverted through the creation of an "HC−FC" surface dipole. Thus, a new series of methyl-capped partially fluorinated alkanethiols, $CH_3(CF_2)_6(CH_2)_nSH$ (where $n$ = 10−13), were designed and synthesized. Structural analyses of the new films show that these adsorbates give rise to well-ordered monolayers. As for the wetting behavior of various liquids on these FSAMs, the new films proved to be less hydrophobic than both the corresponding $CF_3$-terminated and hydrocarbon SAMs and more oleophobic than their hydrocarbon counterparts. Furthermore, odd−even trends were observed in the wettability of the nonpolar and polar aprotic liquids on the new films in which the *even* FSAMs were more wettable than the *odd* ones for both types of liquids. However, an inverse odd−even trend was observed for polar protic liquids: *odd* FSAMs were more wettable than *even*. We attribute this latter effect to the resistance of highly hydrogen-bonded liquid molecules at the liquid−FSAM interface to adopt a more favorable orientation (on the basis of polarity) when in the presence of the inverted HC−FC dipole.

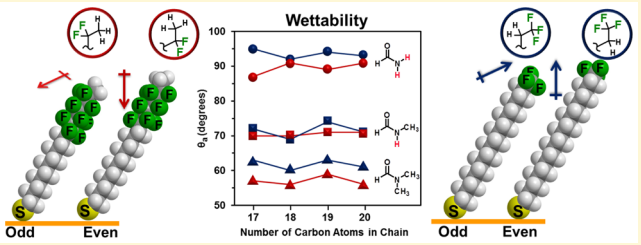


## INTRODUCTION

The ability to decorate the tailgroups of partially fluorinated chains with different functional moieties opens up new avenues for the use of fluorinated amphiphiles as seeds for a new generation of fluorinated materials. Modifications that have created a sandwich of the fluorinated segment, like the recently reported PEG-terminated fluorinated thiols, have given rise to water-soluble partially fluorinated gold nanoparticles.[1,2] Furthermore, the ability to distribute fluorinated moieties spatially within a larger network have led to a better understanding of the influence that such defined levels of fluorination can have upon the larger assembly,[3] with recent examples being the incorporation of perfluorinated aromatic tetrazoles and carboxylic acids in metal organic frameworks (MOFs), creating highly fluorinated MOFs with superhydrophobic character.[4] Separately, research involving fluorinated films has also benefitted from such advancements in organic synthesis; for example, Cai and co-workers have used click chemistry to create microarrays on fluorinated surfaces.[5]

Investigations involving self-assembled monolayers (SAMs) of thiols on gold surfaces continue to serve as model systems for determining how the structural features of fluorinated amphiphiles can be used to tailor the physical and interfacial properties of monolayer films. Fundamental studies of fluorinated self-assembled monolayers, FSAMs, have shown that fluorinated alkanethiols surpass their hydrocarbon analogues in key characteristics such as chemical and biological inertness, thermal stability, and oleo- and hydrophobicity.[6,7] Such properties are inherent in these structures owing in part to the intrinsic characteristics of the C−F bond (extremely polar but with a reported bond strength of 105.4 kcal per mole),[8] as well as the stiff helical geometry of the perfluorinated chains.[9−11] In addition, extended perfluorocarbon chains have a larger surface area as compared to their hydrocarbon counterparts.[12]

More than a decade ago, Lee and co-workers introduced a series of $CF_3$-terminated alkanethiols for thin-film research.[13,14] SAMs derived from these molecules on gold surfaces exhibited similar structural features to their normal alkanethiol counterparts.[15−17] Despite the differences in the sizes of the terminal methyl groups, the underlying alkyl chains appear to possess the same arrangement as the alkyl chains of alkanethiolate SAMs on a gold lattice.[18] However, the interfacial properties reflect the change in the chemical makeup of the tailgroup; the $CF_3$-terminated SAMs are less hydrophobic than normal hydrocarbon SAMs due to the dipole residing at the fluorocarbon−hydrocarbon (FC−HC) junction.[13] Colorado and Lee investigated this phenomenon using a series of $CF_3$-

Received: September 1, 2015
Revised: October 7, 2015
Published: October 9, 2015





DOI: 10.1021/acs.chemmater.5b03411
Chem. Mater. 2015, 27, 7433−7446

terminated SAMs ($CF_3(CH_2)_nSH$, where $n$ = 12−15) in comparison to analogous normal alkanethiolate SAMs.[19] Their study also included FSAMs where the FC−HC dipole was systematically buried into the film by increasing the length of the fluorinated moiety, while keeping the overall chain length constant at 16 backbone carbons ($F(CF_2)_n(CH_2)_mSH$, where $n$ = 1−10 and $m$ = 15−6; F$n$H$m$SH).[19]

These studies indicate that all FSAMs formed from terminally fluorinated thiols are more oleophobic than their nonfluorinated analogues due to the nonideal dispersive interactions between fluorocarbons and hydrocarbons. On the other hand, $CF_3$-terminated SAMs are more wettable by polar liquids than normal alkanethiolate SAMs. Furthermore, the former exhibit an inverse "odd−even" effect by polar aprotic liquids greater in magnitude than that commonly seen with such contacting liquids on normal alkanethiolate SAMs. According to Colorado and Lee, these findings support the presence of the FC−HC dipole in $CF_3$-terminated SAMs, and the orientation of the dipole coincides with the orientation of the terminal perfluoromethyl group. Hence, the total number of carbons in the chain gave rise to an observed "odd−even" effect for polar aprotic contacting liquids that corresponds with the noncompensated strength of the interfacial dipole. Furthermore, burying the FC−HC dipole in the film by increasing the number of terminal fluorocarbons in the F$n$H$m$SH series of FSAMs led to a decrease in the wetting ability of polar liquids on these monolayers. This latter effect was confirmed by another wettability study on a second series of fluorinated SAMs ($F(CF_2)_n(CH_2)_{11}SH$, where $n$ = 1−10; F$n$H11SH), where the wettability of contacting liquids decreased with an increasing length of the terminal perfluorinated segment until the wetting behavior of the contacting liquids plateaued at five fluorocarbons and beyond.[20]

Other interfacial properties of FSAMs, such as adhesion and friction, are also influenced by the chemical nature of the terminal group. For example, fluorinated monolayers exhibit weak adhesive properties;[21−23] however, atomic force microscopy (AFM) studies have shown that $CF_3$-terminated SAMs exhibit a higher coefficient of friction due to the larger van der Waals (vdW) diameter of the terminal group (∼5.6 Å), and that the bulkier chain ends are locked in a confined spatial arrangement due to the efficient packing of the underlying alkyl spacers where the lattice spacing of chains in the two types of films is ∼4.8 Å.[15,18,24]

The current investigation examines the first examples of FSAMs having a reversed interfacial dipole (HC−FC). The $CH_3$-terminated, partially fluorinated alkanethiols featured in this study are of the form $CH_3(CF_2)_6(CH_2)_nSH$ (H1F6H$n$SH; where $n$ = 10−13). *Notably, the type of interface formed from these thiols, a terminally fluorinated SAM capped with $CH_3$ groups, is unprecedented in interfacial science and represents a new class of organic thin film with unknown and unpredicted properties.*[25] The length of the fluorocarbon segment was set at six fluorocarbons in order to minimize the effect of the second "buried" FC−HC dipole, associated with the transition at the underlying alkyl spacer, on the interfacial properties of the resulting monolayers. The number of methylene units in the spacer was set at a minimum of 10 to ensure minimal influence from the underlying gold substrate on contacting liquid wetting behavior and to allow for the generation of monolayers with minimal gauche defects in the hydrocarbon region of the film. Further, we compared the monolayers derived from the H1F6H$n$SH adsorbates to those derived from $n$-alkanethiol (H$x$SH; $x$ = 17−20) and $CF_3$-terminated alkanethiol (F1H$m$SH, where $m$ = 16−19) adsorbates having the same chain lengths (see Figure 1). The properties of the SAMs

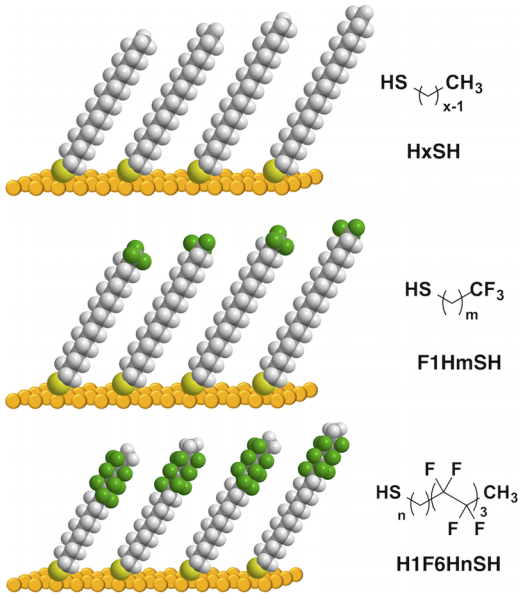


**Figure 1.** Illustrations of the chemisorbed adsorbates associated with the monolayer films formed from the deposition of (top) normal alkanethiols (H$x$SH), (middle) $CF_3$-terminated alkanethiols (F1H$m$SH), and (bottom) methyl-terminated partially fluorinated thiols (H1F6H$n$SH). All of the SAMs were prepared on gold surfaces.

analyzed in this study were characterized using ellipsometry, X−ray photoelectron spectroscopy (XPS), polarization modulation infrared reflection-adsorption spectroscopy (PM-IRRAS), and contact angle goniometry.

## EXPERIMENTAL SECTION

Details of the experimental procedures including materials and chemicals used in this research, synthetic procedures, characterization data of the H1F6H$n$SH and F1H$m$SH molecules, preparation of the gold substrates and the investigated monolayers, and experimental methods used to evaluate the thin films (ellipsometry, XPS, PM-IRRAS, contact angle goniometry, and molecular modeling) are provided in the Supporting Information.

## RESULTS AND DISCUSSION

In this investigation, we compare the new H1F6H$n$SH FSAMs to SAMs derived from normal alkanethiols having an equivalent carbon count in the molecular chain (H$x$SH). The latter SAMs have been rigorously characterized in the literature and provide a point of reference for the complete set of data for the new FSAMs when formed on the same batch of vapor-deposited gold. Additionally, we examine SAMs derived from a series of $CF_3$-terminated alkanethiols (F1H$m$SH) bearing the same number of carbons as the H1F6H$n$SH adsorbates to provide an appropriate comparison of the influence of the unique interfacial dipole of the new FSAMs upon the interfacial properties of the films.

**Ellipsometric Assessment of Monolayer Formation.** To generate SAMs from the newly designed methyl-capped, partially fluorinated alkanethiols (H1F6H$n$SH), we initially examined their development in ethanol for 48 h at room temperature (rt); established literature on fluorinated alkanethiols indicates that ethanol is an appropriate solvent for


DOI: 10.1021/acs.chemmater.5b03411
Chem. Mater. 2015, 27, 7433−7446

**Table 1. Ellipsometric Data for SAMs Formed from Methyl-Capped, Partially Fluorinated Alkanethiols, Normal Alkanethiols, and $CF_3$-Terminated Alkanethiols**[a]

| adsorbate | thickness (Å) | adsorbate | thickness (Å) | adsorbate | thickness (Å) |
|---|---|---|---|---|---|
| H17SH | 21 (21) | F1H16SH | 18 | H1F6H10SH | 17 |
| H18SH | 23 (22) | F1H17SH | 20 | H1F6H11SH | 19 |
| H19SH | 24 (23) | F1H18SH | 21 | H1F6H12SH | 20 |
| H20SH | 25 (25) | F1H19SH | 23 | H1F6H13SH | 21 |

[a]Ellipsometric data are within ±2 Å of the average thickness values shown. Reference values obtained from a prior report are presented in parentheses.[30]

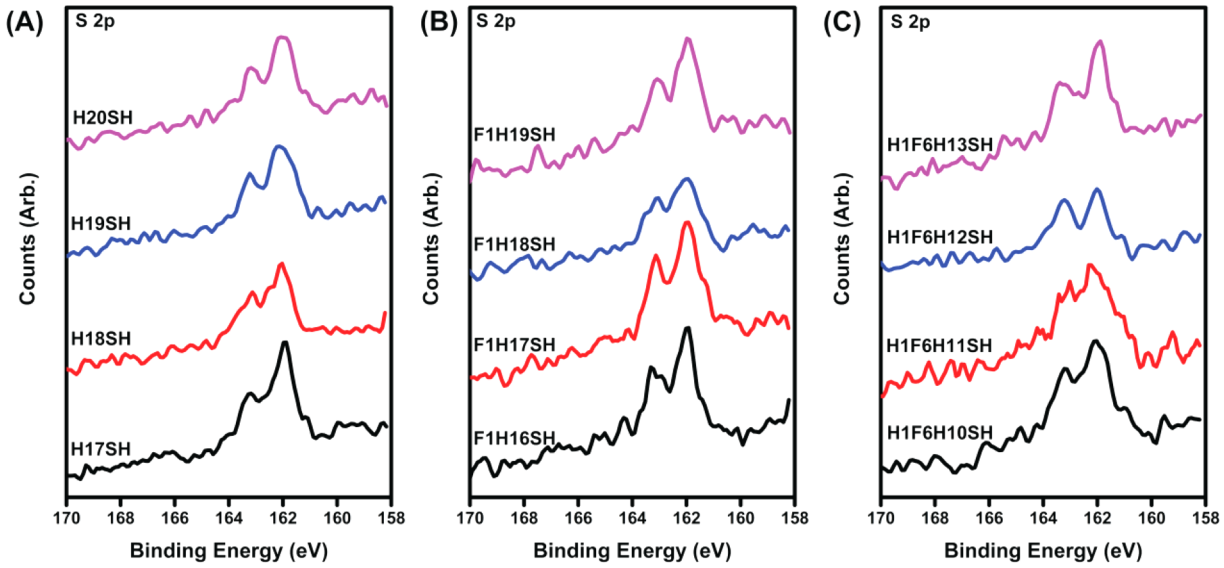


**Figure 2.** XPS spectra for the S 2p region of the investigated SAMs: (A) H*x*SH, (B) F1H*m*SH, and (C) H1F6H*n*SH.

developing related FSAMs.[20] The first set of ellipsometric measurements provided thickness data for the new FSAMs that were short of the anticipated thicknesses, while the other films prepared for this study, monolayers formed from H*x*SH and F1H*m*SH, were in line with anticipated film thicknesses. In efforts to enhance the film thicknesses of the new thiolate adsorbates on gold, we further equilibrated all of the H1F6H*n*SH monolayers for an additional 24 h in ethanol at 40 °C, which enhances the mobility of the thiolate species on the gold surface and, therefore, the final packing density.[26]

The average thicknesses of the fully developed monolayers are shown in Table 1. The average thicknesses of the SAMs generated from the normal alkanethiols (H*x*SH) are within experimental error of the literature values, 21, 22, 23, and 25 Å for the SAMs formed from **H17SH**, **H18SH**, **H19SH**, and **H20SH**, respectively.[26,27] The $CF_3$-terminated SAMs produced average thickness measurements of 18, 20, 21, and 23 Å for the SAMs formed from **F1H16SH**, **F1H17SH**, **F1H18SH**, and **F1H19SH**, respectively. Because prior research into $CF_3$-terminated alkanethiolate SAMs has shown that these adsorbates form films that are generally about ∼1.5 Å shorter than their normal alkanethiolate counterparts, the obtained values appear to be appropriate for these films.[28] On the other hand, the thickness values for the methyl-capped fluorinated thiols were ∼1 Å shorter still (but within experimental error): 17, 19, 20, and 21 Å for the SAMs formed from **H1F6H10SH**, **H1F6H11SH**, **H1F6H12SH**, and **H1F6H13SH**, respectively. The increase in monolayer thickness within the H1F6H*n*SH SAM series, as well as the other two sets of SAMs, is in line with an increase of one methylene unit per homologue in the series (∼1−2 Å per $CH_2$ unit).[27,29]

Although the H1F6H*n*SH films are marginally thinner than the H*x*SH and F1H*m*SH films, the thickness measurements are consistent with those of more highly fluorinated alkanethiolate films (i.e., partially fluorinated FSAMs of the form F*n*H*m*SH).[29,31] Unlike the H1F6H*n*SH FSAMs, however, the terminally fluorinated FSAMs developed well-packed films within 48 h in ethanol at rt.[20,32] The perfluorinated segment for these similarly structured adsorbates has been reported to exhibit a reduced tilt from normal as compared to the hydrocarbon segment; therefore, the film thicknesses were anticipated to be close to their comparative offsets.[31,33] The reduction in film thickness for the H1F6H*n*SH FSAMs as compared to the other SAMs analyzed in this study might reflect a lower chain density. Because of the larger size of a fluorinated helix (with a diameter of 5.6 vs 4.2 Å for a hydrocarbon chain),[34] the fluorinated chains occupy less space on the gold lattice, as was shown previously by AFM.[35] Furthermore, structural studies of SAMs derived from partially fluorinated alkanethiols (F10H*n*SH, where *n* = 11, 17, and 33) found that an increase in length of the alkyl spacer gives rise to some disordering of the fluorinated layer and that the increase in vdW interactions among the methylene spacers gives rise to an increase in tilt for the fluorinated chains.[33,35] The aforementioned reasons could lead to a lower chain density, which corresponds to lower thicknesses for the H1F6H*n*SH FSAMs. In addition, the reduction of the refractive index associated with fluorocarbons (1.33) versus that of hydrocarbons (1.45) might contribute to the observed reduction in


DOI: 10.1021/acs.chemmater.5b03411
*Chem. Mater.* 2015, 27, 7433−7446

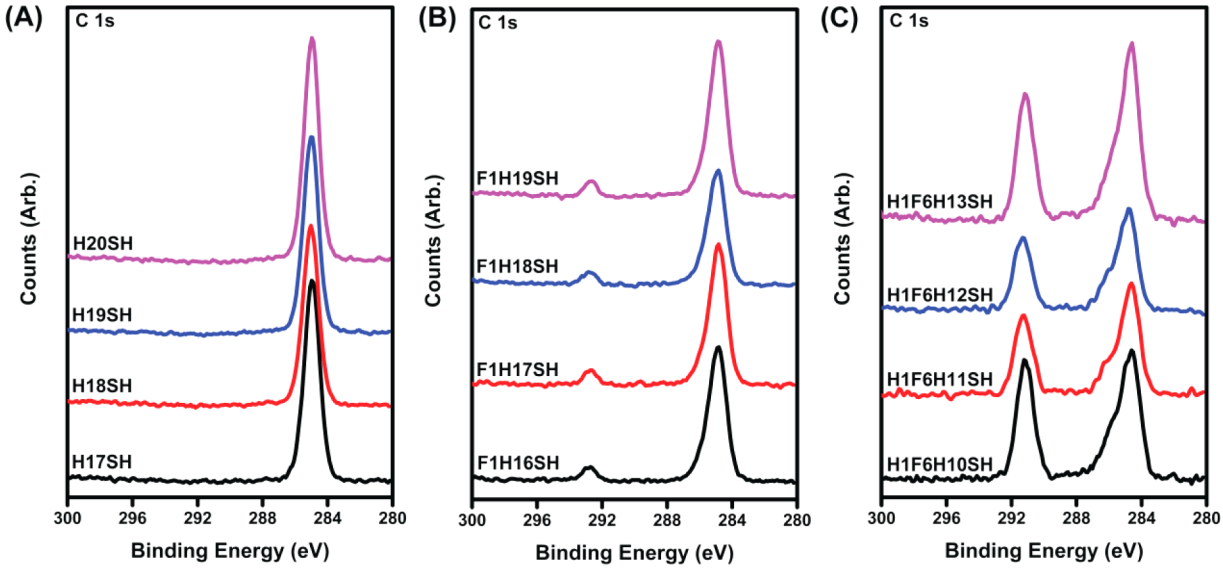


**Figure 3.** XPS spectra for the C 1s region of the investigated SAMs: (A) H*x*SH, (B) F1H*m*SH, and (C) H1F6H*n*SH.

the thickness values for H1F6H*n*SH FSAMs because we used a refractive index value of 1.45 for these films to obtain the ellipsometric thicknesses.[36] Considering these possible contributions to the marginally low thicknesses measured for the H1F6H*n*SH FSAMs, and that the three sets of SAMs were produced from alkanethiols with equivalent carbon counts, the analysis of the film packing characteristics provided in the following section sheds some additional light on the observed differences in film thickness.

**XPS Analysis of the Composition and Packing of the SAMs.** Analysis of SAMs by XPS reveals the chemical nature of the atoms on the surface and provides insight into the structural features of the monolayers.[37] Survey spectra show the presence of only Au, C, F, and S for the H1F6H*n*SH and F1H*m*SH SAMs, while the H*x*SH SAMs only show Au, C, and S. The binding energies of the elements are provided in Table S1. The S 2p region for all the SAMs investigated herein (see Figure 2) reveals that peaks associated with bound sulfur are positioned at ~162 and 163.8 eV. These characteristic peaks have been assigned to the S $2p_{3/2}$ and the S $2p_{1/2}$ binding energies, respectively, for sulfur bound to gold.[38] The absence of peaks at ~164−166 eV, which are the binding energies associated with the sulfur of unbound thiol, indicates that the rinse procedure used to clean the SAMs is sufficient to remove unbound thiol from the surface. In addition, a successful rinse procedure ensures that the thickness values discussed in the earlier section are representative of monolayers bound to the gold surface.

Aside from determining the chemical composition of a monolayer, XPS analysis can be used to examine qualitatively the chain density of the molecules that form a monolayer. Figure 3 shows the C 1s region of all SAMs prepared for this study. The C 1s spectra of the H1F6H*n*SH FSAMs reveal two large peaks characteristic of $CF_2$ and $CH_2/CH_3$ units.[33,35] On the other hand, the spectra of H*x*SH SAMs show only one peak (i.e., that associated with the $CH_2/CH_3$ units), and the SAMs formed from F1H*m*SH show two peaks characteristic of $CF_3$ and $CH_2$ units. Comparison of the position of the C 1s peaks corresponding to the hydrocarbons (see Table S1) shows that the corresponding values for this peak in the H1F6H*n*SH FSAMs are shifted to a lower binding energy (~284.6 eV) as compared to those of the H*x*SH (~285.0 eV) and F1H*m*SH (~284.9 eV) SAMs. Such a shift in binding energy can be correlated to changes in the packing density of the alkyl chains on the gold surface.[39] This observation is in line with the increased vdW diameter of the fluorinated helix as compared to the hydrocarbon chain, a difference in structure that can cause such adsorbates to occupy a larger space on the gold lattice as opposed to that occupied by a normal alkanethiolate or $CF_3$-terminated alkanethiolate adsorbate.[15,21,35] It has been previously observed in monolayer films of chains that are similar in chemical structure that well-packed films act as good insulators, which hinders the processes of discharging positive charges generated by XPS irradiation, which translates to an increase in the binding energy of their emitted electrons; on the other hand, loosely packed chains behave as poor insulators.[35,40,41] Additionally, the binding energy of the C 1s peak for the $CH_2$ units for the H1F6H*n*SH series falls within the same range for all the generated films. The consistency in the peak position of the C 1s peak for the $CH_2$ units of the H1F6H*n*SH FSAMs indicates the formation of a well-packed monolayer for this type of adsorbate having at least 10 methylene ($CH_2$) units in the backbone. Further, analysis of the F 1s XPS spectra of the H1F6H*n*SH series in Figure S21 also indicates that the perfluorinated segments of these monolayers share similar packing densities—a conclusion supported by the consistency of the binding energy values for the F 1s core electrons of the $CF_2$ units in the films, as outlined in the Supporting Information. Taking into account all of the collected XPS data, the chains in the H1F6H*n*SH FSAMs appear to possess a lower packing density vis-à-vis those in the H*x*SH and the F1H*m*SH monolayers, and there is no apparent enhancement in packing density in the H1F6H*n*SH FSAMs as a function of the number of methylene units for the adsorbates examined in this study.

**PM-IRRAS Analysis of the Relative Conformational Order of the SAMs.** The relative conformational order and chain orientation for alkanethiolate self-assembled monolayer films can be evaluated using surface IR. The conformational order (or crystalline nature) of SAMs can be most easily estimated from the position of the antisymmetric methylene C−H stretching band ($\nu_{as}^{CH_2}$).[42−44] The appearance of this band at ~2918 $cm^{-1}$ is an indication of a well-ordered (or


DOI: 10.1021/acs.chemmater.5b03411
*Chem. Mater.* 2015, 27, 7433−7446

relatively "crystalline") monolayer with the alkyl moieties adopting a largely all-*trans*-extended conformational alignment, similar to that of paraffin wax. However, shifts in the position of this band to a higher wavenumber indicate a less-ordered SAM having gauche defects. Figure 4 shows the PM-IRRAS spectra for the C−H stretching region of the SAMs studied herein. Figure 4A shows the H*x*SH SAMs with a $\nu_{as}^{CH_2}$ band at 2918 $cm^{-1}$, consistent with a monolayer having *trans*-extended chains.[4,44]

The H1F6H*n*SH FSAMs also exhibit a $\nu_{as}^{CH_2}$ band at 2918 $cm^{-1}$ (Figure 4C), which is consistent with the results from previous IR studies of F*n*H11SH FSAMs and with the SAMs in this study formed from F1H*m*SH, as shown in Figure 4B.[20,45] On the basis of the above-mentioned spectra and the values listed in Table S2, the conformational order of the hydrocarbon spacer of the H1F6H*n*SH FSAMs is as crystalline in nature as the alkyl chains of the other SAMs. Note that the dynamic feature in the PM-IRRAS spectra of the H1F6H*n*SH SAMs is the increase in the intensity of the $\nu_{as}^{CH_2}$ band as the number of the underlying methylene units increases, which is an expected result. The subtle odd−even trends apparent in comparisons of the C−H stretching vibration bands, especially the methyl C−H stretches in the H*x*SH series, are discussed in the Supporting Information. It must be noted, however, that we are unable to detect these bands with absolute certainty in the PM-IRRAS spectra of the H1F6H*n*SH FSAMs. A minor shoulder at ∼2960 $cm^{-1}$ is present for three of the films but is not discernible in the SAM formed from **H1F6H11SH**. We also observe intrinsic weaknesses for both the $\nu_{s}^{CH_3}$ and $\nu_{as}^{CH_3}$ modes in the transmission IR spectra collected for the H1F6H*n*SH compounds (see Figure S22 in the Supporting Information). The apparent diminution of these vibrations reflects the influence of the fluorocarbon chain segment on the methyl C−H bonds. Similar results can be found in the work of Durig and co-workers, who conducted research on 2,2-difluorobutane.[46] This short alkane possesses a methyl group adjacent to the fluorocarbon and one that is positioned $\beta$ to the fluorinated moiety. For this compound, the authors found that the $\nu_{as}^{CH_3}$ peak was weak for the adjacent methyl group but strong for the one that was separated from the fluorocarbon by one methylene. For our report, the poor resolution of the $\nu_{s}^{CH_3}$ and $\nu_{as}^{CH_3}$ bands precludes a direct odd−even comparison between the H*x*SH and H1F6H*n*SH series.

**Contact Angle Study of the Interfacial Properties of the SAMs.** *Parameters Used in the Study and Wettability Trends.* Highly fluorinated surfaces enjoy an extremely low surface energy that manifests in their high degree of repellency toward both water and oil.[6,7,47] These features have motivated surface scientists to incorporate fluorinated chains into a variety of materials in an effort to minimize interfacial energy, thereby creating surfaces with low adhesion and coefficients of friction.[22,23] Accordingly, FSAMs formed from terminally fluorinated alkanethiols have been used to study the effect of fluorination on surface wettability and ultimately control its impact. This research led to the conclusion that the dipole associated with the fluorinated end of the adsorbates used to generate $CF_3$-terminated SAMs causes the surfaces to be less hydrophobic than those of normal alkanethiolate SAMs when that FC−HC dipole is in close proximity to the interface.[13,19,20] To expand upon the aforementioned knowledge regarding the role of an interfacial dipole to include that of an HC−FC dipole on surface interfacial energy, we examine here the wettability of FSAMs formed from the H1F6H*n*SH molecules toward a

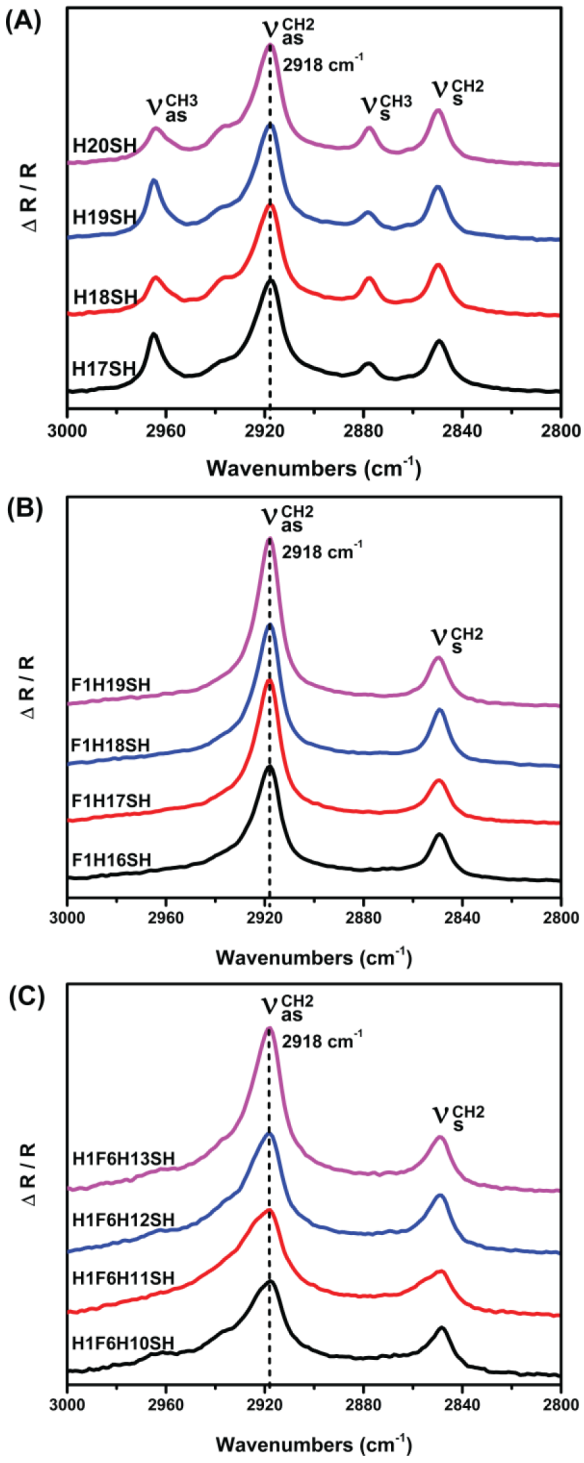


**Figure 4.** PM-IRRAS spectra for the C−H stretching region for SAMs generated from the adsorption of (A) H*x*SH, (B), F1H*m*SH, and (C) H1F6H*n*SH on gold surfaces. SAMs of H*x*SH and F1H*m*SH serve as reference films for the H1F6H*n*SH SAMs for interpreting the C−H stretching vibration spectra. Note that changes in the peak intensities in the H*x*SH spectra associated with odd−even effects are fully described in the Supporting Information.

variety of contacting liquids, including polar protic liquids (water ($H_2O$), $\gamma_{LV}$ = 72.8 mN/m; glycerol (GL), $\gamma_{LV}$ = 65.2 mN/m; and formamide (FA), $\gamma_{LV}$ = 57.3 mN/m),[48−50] polar aprotic liquids (nitrobenzene (NB), $\gamma_{LV}$ = 43.8 mN/m; dimethyl sulfoxide (DMSO), $\gamma_{LV}$ = 43.5 mN/m; and


DOI: 10.1021/acs.chemmater.5b03411
*Chem. Mater.* 2015, 27, 7433−7446

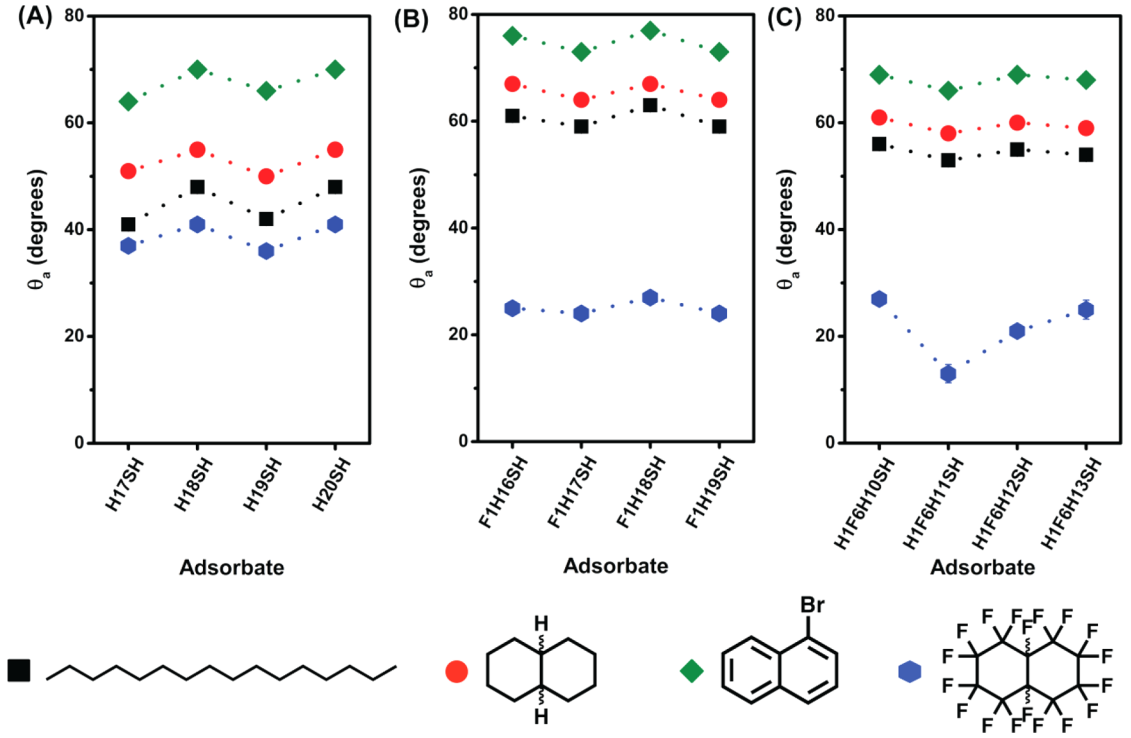


**Figure 5.** Advancing contact angle values for HD, DC, BNP, and PFD on monolayers derived from (A) H*x*SH, (B), F1H*m*SH, and (C) H1F6H*n*SH formed on gold. Lines connecting the data points are simply guides for the eye. *Error bars that are not visible fall within the symbols.*

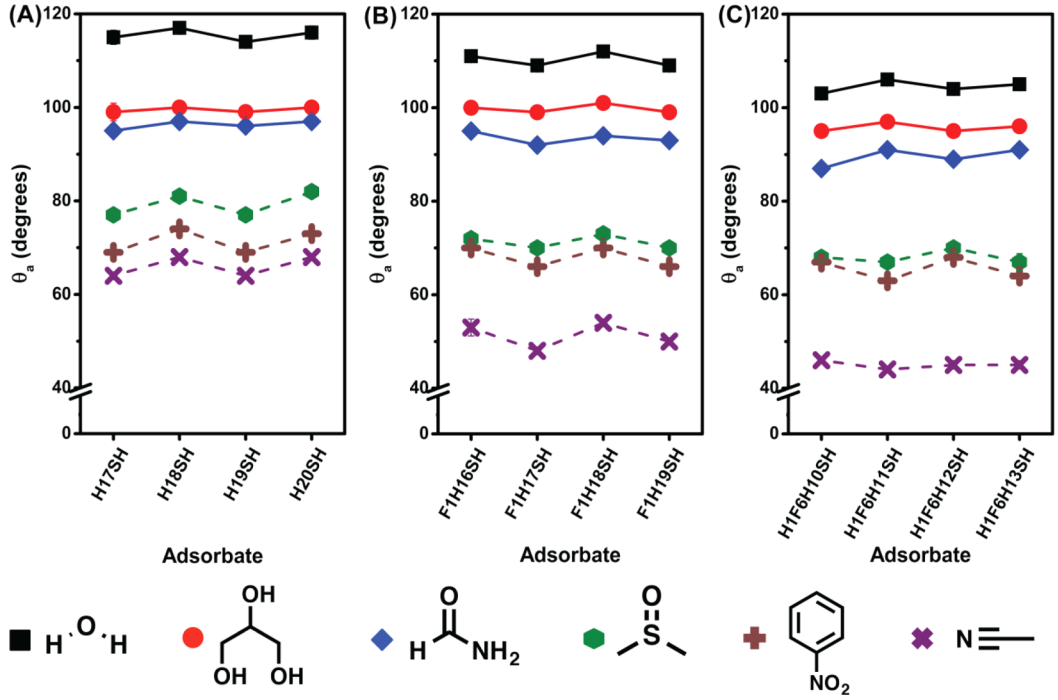


**Figure 6.** Advancing contact angle values for $H_2O$, GL, FA, DMSO, NB, and ACN on SAMs derived from (A) H*x*SH, (B), F1H*m*SH, and (C) H1F6H*n*SH formed on gold. Lines connecting the data points are simply guides for the eye. *Error bars that are not visible fall within the symbols.*

acetonitrile (ACN), $\gamma_{LV}$ = 28.7 mN/m),[49,50] and a bulky hydrocarbon liquid with a small localized dipole (bromonaphthalene (BNP), $\gamma_{LV}$ = 44.6 mN/m).[51] We also probed the new FSAMs with nonpolar contacting liquids, including liquids formed from a long alkyl chain (hexadecane (HD), $\gamma_{LV}$ = 27.1 mN/m),[49] a bulky bicyclic hydrocarbon (decalin (DC), $\gamma_{LV}$ = 29.4 mN/m (trans); 31.7 mN/m (cis)),[49] and a bulky bicyclic perfluorocarbon (perfluorodecalin (PFD), $\gamma_{LV}$ = 19.2 mN/m).[50] The corresponding advancing contact angle values are presented in Tables S3 and S4 in the Supporting Information, where they are compared to the advancing contact angle data for the SAMs formed from H*x*SH and F1H*m*SH. The advancing contact angle data for the H*x*SH SAMs show that *n*-alkanethiolate SAMs with an even number of carbons in their



DOI: 10.1021/acs.chemmater.5b03411
*Chem. Mater.* 2015, 27, 7433−7446

chains (**H18SH** and **H20SH**) are less wettable than those with an odd number (**H17SH** and **H19SH**), which is consistent with observations reported in the literature.[19] This phenomenon is largely due to the orientation of the terminal methyl group, which is more aligned with the surface normal in SAMs with even-numbered adsorbates (*even*) than those with odd-numbered adsorbates (*odd*).[37,52] For the *odd n*-alkanethiolate films, the methyl group is tilted away from the surface normal, exposing the underlying methylene unit to the SAM−liquid interface, which translates to a greater degree of molecular contact between the contacting liquid and the interface.[53] Accordingly, this attractive interaction causes the films formed from *odd* chains in these SAMs to be more wettable than the ones formed from *even* chains, as displayed in Figure 5 (as well as in Figure 6; vide infra).

Prior to analyzing the contact angle data for the three series of SAMs, we had anticipated an increase in wettability for the F1H*m*SH SAMs by polar liquids, as compared to that of the H*x*SH SAMs, owing to the presence of the FC−HC dipole at the interface of the film—the result of permanent dipole−dipole interactions (i.e., Keesom forces) operating at the contacting liquid−SAM interface. However, unlike our initial studies on $CF_3$-terminated SAMs with shorter underlying alkyl chains,[13,54] the data in Table S3 show that there is also a well-defined odd−even trend for our nonpolar contacting liquids when in contact with the F1H*m*SH SAMs that is inverse to that of the H*x*SH SAMs. For nonpolar contacting liquids on these films, the SAMs formed from the *even* chains are more wettable than those formed from the *odd* chains. According to Colorado and Lee, for polar contacting liquids this phenomenon is caused by the orientation of the terminal $CF_3$ group (vide supra), which is directed toward the contacting liquid in SAMs with *even* chains and away from it in SAMs with *odd* chains.[19,20] However, when using PFD, a nonpolar perfluorocarbon liquid, as the contacting liquid, an odd−even effect can also be observed. This trend might be attributed to the phase-compatible interactions between fluorinated compounds and appears to be directly related to the number of fluorine atoms interacting with the liquid at the SAM−liquid interface. Thus, films with *even* chains whose terminal groups are more aligned with the surface normal are more wettable than those with *odd* ones. On the other hand, the odd−even effect observed in the wettability data for the F1H*m*SH films with nonpolar hydrocarbon liquids, exhibited in Figure 5, complicates the aforementioned interpretation of the PFD data, leading to a conclusion that the interactions of all of the nonpolar contacting liquids must be considered more carefully. In particular, the contacting liquids that interact with the SAM interface might be responding to an increase in surface tension (surface energy) associated with having an increase in electron density at the monolayer interface—a result of the $CF_3$ termini being oriented almost parallel to the surface normal. This orientation was determined by an analysis of the angle of the final carbon−carbon bond, which we calculated to have a tilt angle of ∼17° from the surface normal using molecular modeling as shown in Figure S26 in the Supporting Information (i.e., the *even* chains support a permanent dipole−induced dipole interaction or "Debye force" between the SAM and the contacting liquid, respectively). On the other hand, having the $CF_3$ termini tilted away from the interface, as is the case with the odd-numbered chains (∼58° from the surface normal, as illustrated in the Supporting Information), allows compensating head-to-tail interactions between the dipoles in the SAMs, which reduces the magnitude of the aforementioned dipole−induced dipole interaction between the SAM and the contacting liquid, leading to a reduction in wettability.

*Effects of H1F6HnSH Structure/Composition on the Interfacial Properties.* To evaluate the role of structure/composition on the surface energy of the partially fluorinated monolayers generated by the introduction of the methyl termini on top of the perfluorinated segment, we first examined the contact angle data for nonpolar contacting liquids on the H1F6H*n*SH FSAMs. The contact angle measurements obtained for liquids whose surface interactions are dominated by dispersive forces (HD and DC) on the H1F6H*n*SH films indicate that the chains are well-packed, as also determined by the IR analysis (vide supra). This hypothesis was confirmed by the contact angle values of hexadecane (see Figure 5), which appear to indicate that this contacting liquid fails to intercalate between the chains of the H1F6H*n*SH FSAMs. Furthermore, the wettability data of decalin (a bulky hydrocarbon liquid) and hexadecane on the 18-carbon chain of the $CH_3$-terminated film (**H1F6H11SH**: 58° and 53°, respectively) show that this FSAM is more oleophobic than the normal alkanethiolate counterpart (**H18SH**: 55° vs 48°, respectively). A driving force for this phenomenon could be the underlying perfluorocarbon segment, which lies almost at the interface, along with the steric bulk of the perfluorocarbons, which plausibly reduces the intercalation of liquid molecules within the chain assembly. In the H1F6H*n*SH monolayer system, the smaller $CH_3$ groups on top of the larger fluorocarbon helix would also contribute to the underlying $CF_2$ units interacting with liquids in contact with these FSAMs, which would lead to a reduced wetting behavior for hydrocarbon liquids on the H1F6H*n*SH FSAMs due to the nonideal dispersive interactions between hydrocarbons and fluorocarbons, similar to the observed wettability trends of these liquids on the F1HmSH films compared to the HxSH films. In addition, the contact angle data of perfluorodecalin on the H1F6H*n*SH FSAMs suggest that the underlying fluorinated chain contributes to the interfacial energy; in particular, note that H1F6H*n*SH films are more wettable by PFD than are the H*x*SH SAMs, and they exhibit similar wetting behavior toward PFD as the F1H*m*SH SAMs. However, complicating our interpretation is an obvious dip in the contact angle data of PFD on the **H1F6H11SH** FSAM, which might reflect a combination of influences: the low surface tension of PFD (19.2 mN/m)[50] accompanied by a reduction in chain packing for the FSAM in question. Notably, we observed a similar trend in contact angle data for the H1F6H*n*SH FSAMs when we tested a different low surface tension liquid (*t*-butyl alcohol, $\gamma_{LV}$ = 21.1 mN/m),[49] as shown in Figure S23 in the Supporting Information.

To evaluate the role of the inverted dipole (HC−FC), we first compare the wettability of polar contacting liquids on the newly designed H1F6H*n*SH FSAMs to that on the H*x*SH and F1H*m*SH SAMs (see Figure 6). Most obviously, the values for the advancing contact angles for the polar liquids are uniformly lower on the H1F6H*n*SH films than on those formed from H*x*SH and F1H*m*SH. More specifically, the H1F6H*n*SH FSAMs are far more wettable than the H*x*SH series when in contact with the polar aprotic liquids DMSO and ACN and are slightly more wettable than the F1H*m*SH SAMs. Further, the trends in the data for the polar liquids on the H1F6H*n*SH FSAMs (Figure 6C) appear to be more similar to the trends on the F1H*m*SH SAMs (Figure 6B) than those on the H*x*SH


DOI: 10.1021/acs.chemmater.5b03411
*Chem. Mater.* 2015, 27, 7433−7446

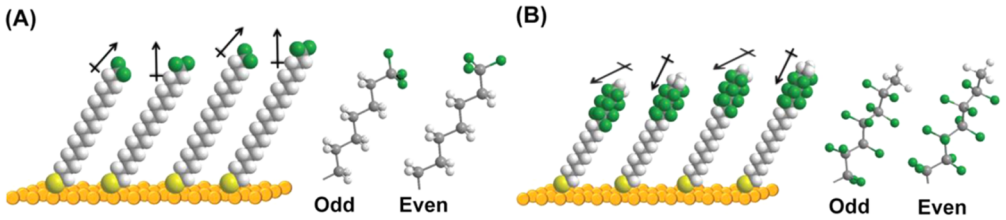


**Figure 7.** Illustration of the orientation of the methyl and trifluoromethyl termini in SAMs derived from the adsorption of (A) F1H*n*SH and (B) H1F6H*n*SH on gold. Molecular modeling of the thiols was performed using the ORCA program package, as described in the Supporting Information.

SAMs (Figure 6A). The data for the H1F6H*n*SH FSAMs are consistent with a model in which the $CH_3$-capped, partially fluorinated alkanethiolate FSAMs are more wettable than their normal alkanethiolate counterparts due to the presence of a dipole at the HC−FC termini (i.e., Keesom forces appear to be at play for the FSAMs).

Other effects, however, appear to be in play as well. More specifically, the differences in the wettability trends of the polar contacting liquids on the H1F6H*n*SH and F1H*m*SH SAMs likely also reflect the influence of the chemical composition of the terminal methyl group, as well as the spatial arrangement of the outer atomic layer at the liquid−solid interface. Although the $CF_3$ groups in SAMs formed from F1H*m*SH are tightly packed, the $CH_3$ termini of the H1F6H*n*SH FSAMs are likely loosely packed owing to the larger vdW radii of the underlying perfluorinated segments (vide supra).[15,21,35] Therefore, smaller probe liquids can readily surround the terminal methyl group, the outermost layer of the monolayer, leading to an increase in wetting for small polar molecules on H1F6H*n*SH films (e.g., 103° for $H_2O$ and 46° for ACN on the **H1F6H10SH** SAM) as compared to F1H*n*SH films (e.g., 111° for $H_2O$ and 53° for ACN on the **F1H17SH** SAM). By examining the wettability data for BNP and NB (bulky liquids with a localized dipole), there seems to be support for this "intercalation" model. The inability of either BNP or NB to intercalate below the outermost methyl layer reduces the interaction of the dipole of these liquids with the surface dipoles in the H1F6H*n*SH films, thus giving both liquids similar contact angle values on these FSAMs (i.e., 66° for BNP and 63° for NB on the **H1F6H11SH** SAM). In contrast, the contact angle values of these liquids differ significantly on F1H*m*SH FSAMs, where NB, a liquid with a stronger dipole (4.22 D),[55] wets these monolayers more than BNP (1.55 D)[56] (i.e., 73° for BNP and 66° for NB on the **F1H17SH** SAM). Nonetheless, the H1F6H*n*SH films are still more wettable toward BNP and NB than are the F1H*n*SH films. This difference is likely due to the difference in the chemical nature of the terminal group, where the $CF_3$ units in the **F1H17SH** SAMs lead to nonideal dispersive interactions between the fluorocarbons in the film and the hydrocarbon-based contacting liquids.

*Odd−Even Effects of Polar Aprotic and Nonpolar Liquids on the H1F6HnSH FSAMs.* The inclusion of a systematic series of H1F6H*n*SH adsorbates to the library of SAMs evaluated herein provides insight into the unique interfacial wettabilities of these newly derived SAMs due to either the number of methylenes in the alkyl spacer, the total number of carbons present in the H1F6H*n*SH chains, or the structural variation at the interface. In earlier sections, evaluations of the underlying methylene units have shown that the hydrocarbon moieties in all H1F6H*n*SH FSAMs possess similar packing densities and crystalline structure. Further, the wettability data in Tables S3 and S4 indicate that, for these new organic films, the *even* monolayers (**H1F6H11SH** and **H1F6H13SH**) are more wettable than the *odd* films (**H1F6H10SH** and **H1F6H12SH**) for all nonpolar hydrocarbon liquids and polar aprotic liquids examined in this study. On the basis of the XPS and IR data discussed in earlier sections, the alkyl chains in the H1F6H*n*SH FSAMs exhibit similar packing densities, and the alkyl segments are also well-ordered for all of these monolayers. In addition, the relatively low hysteresis values ($\theta_a - \theta_r$) of all the contacting liquids on each series of adsorbates, as shown in Tables S5 and S6, are consistent with a model of little or no reordering of the adsorbate chains during the contact angle measurements. Yet there is a clear effect related to the total number of carbons on the structural arrangement of the methyl termini at the monolayer interface—a consequence of the underlying alkyl chain length (*odd* or *even*) on the orientation of the terminal group. While the effect is not as straightforward as that found with the *trans*-extended thiolate SAMs observed in earlier studies,[13,19] the positioning of the methyl terminus of the perfluorinated chain should follow the helicity of the perfluorocarbon chain, and the orientation of this segment should reflect the alignment of the underlying alkyl chain. Thus, the fluorinated segment, with a half-turn helix at six fluorocarbons, will likely give rise to a terminal $CH_3$ unit being oriented at the interface differently from that of the terminal $CF_3$ unit at the interface of a *trans*-extended alkanethiolate chain, as illustrated in Figure 7. Therefore, the observed odd−even effect will have contributions from several factors: changes in the orientation of the terminal $CH_3$ group at the interface of the H1F6H*n*SH FSAMs due to the change in the number of underlying $CH_2$ units, the nature of the exposure of the underlying fluorocarbons at the film interface, and the orientation of the final $CH_3$−$CF_2$ bond as dictated by the small helical twist associated with the six perfluorocarbon moieties.

In the case of the nonpolar liquids HD and DC in Figure 5 and Table S3, the odd−even effect portrayed by the wettability data on the H1F6H*n*SH FSAMs follows the trend observed in earlier wettability studies on $CF_3$-terminated monolayers.[13,54] The exposure of the underlying perfluorinated segment toward the interface for the H1F6H*n*SH films varies systematically with the number of the underlying methylene units in the spacer. Therefore, in the case of the *odd* chains, the increased exposure of the perfluorinated unit at the liquid−SAM interface, as compared to the *even* chains, leads to a slightly lower value in the contact angle of the respective liquid on the even films compared to the odd ones (for **H1F6H11SH** and **H1F6H13SH**: HD = 53° and 54° and DC = 58° and 59°, versus for **H1F6H10SH** and **H1F6H12SH**: HD = 56° and 55° and DC = 61° and 60°). Notably for DC, the possibility of wetting anomalies due to liquid intercalation is minimal due to the bulkiness of the liquid molecules; therefore, the observed


DOI: 10.1021/acs.chemmater.5b03411
*Chem. Mater.* 2015, 27, 7433−7446

odd−even effect most likely arises from differences in the attractive dispersive forces between the hydrocarbon liquid and the methyl termini and the nonideal dispersive forces between the hydrocarbon liquid and the underlying perfluorinated segment.

Regarding the data in Figure 6 and Table S4 for the H1F6H*n*SH SAMs, we focus first on the trends observed for the polar *aprotic* liquids (i.e., DMSO, NB, and ACN). Notably, the validity of the hypothesis described above is reinforced by the odd−even effect in the wettability data observed for these liquids. As with the $CF_3$-terminated films, we use the orientation of the final carbon−carbon bond (the HC−FC transition) as a means of estimating the orientation of the interfacial dipole. In this case, the liquids wet *even* films more than *odd* ones. According to our models in the Supporting Information, the terminal methyl group is aligned more toward the interface in the case of films with *even* chains (∼19° tilt angle from surface normal for the terminal carbon−carbon bond), which corresponds to the HC−FC surface dipole being aligned more toward the interface (and thus largely uncompensated); for the *odd* chains, the HC−FC surface dipole is aligned more parallel with the interface with a calculated tilt angle of ∼79°, as shown in Figure S27 (and thus largely head-to-tail compensated). We note that an analogous effect is revealed by the wetting behavior of polar aprotic liquids on the F1H*m*SH SAMs, where the tilt angles for the terminal carbon−carbon bonds are predicted to be ∼17° and ∼58° for the even and odd chains, respectively, as shown in Figure S26. However, the two series differ in that the odd−even effect in the case of small liquids (e.g., ACN) is less pronounced on the H1F6H*n*SH films as compared to the F1H*m*SH films. A possible rationalization for the difference might be that small liquid molecules are able to intercalate into the H1F6H*n*SH films beyond the methyl termini; this model is supported by the observation that NB (a bulky liquid with a strong dipole) shows a similar trend in the contact angle values for *odd* and *even* surfaces on both types of films.

*HC−FC Dipole Versus the Intermolecular H-Bonding of Polar Protic Contacting Liquids.* Next, we focus on the wettability trends in Figure 6 and Table S4 derived from the polar *protic* liquids (i.e., $H_2O$, GL, and FA) in contact with the H1F6H*n*SH SAMs. To our surprise, the wettability data for these liquids show an odd−even effect that is opposite of that observed in the wettability data of the polar *aprotic* liquids on these SAMs. Specifically, $H_2O$, GL, and FA show a higher value on *even* films (**H1F6H11SH** and **H1F6H13SH**) than on *odd* ones (**H1F6H10SH** and **H1F6H12SH**). This effect is also the opposite of that observed in the wettability data of these liquids on the F1H*m*SH SAMs. Since both types of SAMs (F1H*m*SH and H1F6H*n*SH) show similar trends with polar aprotic liquids, we attribute these changes, at least in part, to the orientation of the SAM interfacial dipole (FC−HC for F1H*m*SH and HC−FC for H1F6H*n*SH). Notably, earlier studies on $CF_3$-terminated systems have shown that the negative charge density of the interfacial dipole of the $CF_3$−$CH_2$ moiety is associated with the fluorinated end of the molecule.[57] Therefore, the HC−FC dipole at the $CH_3$−$CF_2$ junction should also be oriented so that the more electronegative aspect (the perfluorinated segment) of the molecule is associated with the negative end of the dipole. To verify these assumptions, we constructed models to depict the chain termini of the F1H*m*SH and H1F6H*n*SH adsorbates derived from molecular modeling described in the Supporting Information; the differing dipole orientations are illustrated in Figure 7 (see also Figures S24 and S25). Such a difference in the intramolecular direction of the dipole gives rise to a partial positive charge at the interface of the H1F6H*n*SH films and a partial negative charge at the interface of the F1H*m*SH SAMs.

These efforts notwithstanding, the structure of the chain termini at the SAM interface alone cannot rationalize the contrasting trends for the polar protic and polar aprotic liquids. We propose an analysis of the interfacial organization of polar protic liquids with extensive hydrogen bonding (H-bonding) networks, with an example being that of water. Prior research that intended to elucidate the nature of the intermolecular interactions of interfacial water molecules provides an understanding of how hydrogen bonds dictate the orientation of the water molecules at the liquid−vapor interface and create an outer layer of molecules that are predominantly oriented with a free −OH group pointed toward the vapor phase.[58,59] A review by Shen and Ostroverkhov provides perspective and detailed discussions regarding the orientation of water molecules at interfaces.[60] In a study focused on the interfacial region between water and carbon tetrachloride ($CCl_4$), Scatena et al. also found that water molecules arrange with −OH groups oriented toward the outer shell of the H-bonding network at the $H_2O$−$CCl_4$ interface.[61] This orientation has been interpreted to indicate the presence of weak hydrogen bonds with the chlorine atoms of $CCl_4$, but it could also be an indication that the positive ends of the water molecular dipoles were locally orienting with the negative ends of the Cl−C dipoles. However, such a molecular orientation for water on the H1F6H*n*SH films would lead to an arrangement that gives rise to an unfavorable interfacial interaction between the dipoles of the protic liquid ($\delta^+$) and that of the HC−FC dipoles ($\delta^+$) of the chain termini of the H1F6H*n*SH FSAMs. If the strength of the underlying H-bonding network maintains this geometrical arrangement for the surface molecules of the contacting liquid, with the free −OH groups or the positive end of their molecular dipole oriented outward with respect to the drop, this unfavorable interaction would provide impetus for rearrangement of the interfacial water molecules of the liquid drop when in contact with a surface exposing an array of HC−FC dipoles. When rearrangement fails to occur because of H-bonding, then repulsive polar interactions exist at the interface. Such circumstances might lead to a reduction in the wettability by water on monolayers where the surface dipoles are oriented more toward the liquid interface and more closely aligned with the surface normal. This interpretation is supported by the data in Figure 6, which show higher contact angle values for water on the *even* H1F6H*n*SH films as compared to the *odd* ones.

On the other hand, when working with this current model for water in contact with our FSAMs, such strains upon the H-bonding network are unlikely for water in contact with the $CF_3$-terminated films because the latter interfaces expose an array of interfacial dipoles oriented with their negative ends toward the contacting liquid—an array of FC−HC dipoles. Neither is there a sufficient barrier for the interfacial molecules of polar aprotic contacting liquids to reorient on the surfaces of the H1F6HnSH films, owing to the absence of an extensive H-bonding network that would deter such interfacial reordering. This interpretation is also supported by the data in Figure 6, which show lower contact angle values for DMSO on the *even* H1F6H*n*SH films as compared to the *odd* ones.

To provide further insight into the wettability of the H1F6H*n*SH FSAMs, we pursued a series of tests to determine


DOI: 10.1021/acs.chemmater.5b03411
*Chem. Mater.* 2015, 27, 7433−7446

the influence of the H-bonding network within the three polar protic contacting liquids that exhibited inverse trends in Figure 6C: (1) water, by adding ions to interrupt the hydrogen-bonding network of water through a comparison of wettability by water versus brine; (2) glycerol, by systematically varying the molecular structure of glycerol by decreasing the number of −OH groups and increasing the steric bulk to interfere with hydrogen bonding within the liquid (i.e., comparing the wettability by glycerol to that by 1,3-propanediol, isopropanol, 2,4-pentanediol, and cyclohexanol); and (3) formamide, by systematically decreasing the hydrogen-bonding capacity of formamide through a comparison of wettability by formamide (FA) to that by methylformamide (MFA) and dimethylformamide (DMF). The pursuit of these tests starts with the assumption that if the highly hydrogen-bonded liquids that we first tested each preferentially orient with their more electronegative element(s) toward the center of the liquid drop (via the negative end of their molecular dipoles), then it is likely that most liquids that form extensive H-bonding networks will also orient in a similar manner.

*Water Versus Brine.* Figure 8 shows the contact angles of water and brine on the F1H*m*SH and H1F6H*n*SH films; notably, brine fails to show the odd−even trend exhibited by water on the H1F6H*n*SH films. Previous studies of aqueous salt solutions and the structural interactions within the associated liquid drops have shown that the interfacial region of the liquid has a higher concentration of anions compared to the bulk, which weakens the H-bonding networks.[62] Further, the concentration of anions in the interfacial region of brine can plausibly lead to an enhanced interaction between the liquid and the HC−FC dipoles in the even H1F6H*n*SH SAMs, whose dipoles are oriented roughly normal to the surface. We propose that this interaction is responsible for negating the odd−even trend seen for water. Importantly, the wettability of brine on the F1H*m*SH SAMs (which exposes an FC−HC dipole that is repulsive to the anions in brine) exhibits the same trend as water. Furthermore, the H1F6H*n*SH series is more wettable than the F1H*m*SH series toward both water and brine, and brine exhibits higher contact angles than water on both sets of SAMs. The former observation is likely due to the structure/composition of the interface of the H1F6H*n*SH FSAMs, as discussed earlier. On the other hand, the latter observation likely arises from an increase in interfacial surface tension within the liquid (water vs brine) associated with the fact that the charged ions produce stronger intermolecular attractions than that associated with H-bonding.

*Glycerol and Its Analogues.* Figure 9 shows the contact angles of glycerol and systematically chosen analogues having either increasing steric bulk—2,4-pentanediol and cyclohexanol ($\gamma_{LV}$ = 33.4 mN/m)[49]—or decreasing numbers of hydroxyl groups relative to the alkyl component—1,3-propanediol ($\gamma_{LV}$ = 47.4 mN/m) and isopropanol ($\gamma_{LV}$ = 21.7 mN/m). On the H1F6H*n*SH FSAMs, both of the liquids with two −OH groups, 1,3-propanediol and 2,4-pentanediol, failed to produce any odd−even trend. We interpret these results to indicate that the H-bonding networks within the interfacial region of these liquids are disrupted sufficiently to allow minor interfacial molecular rearrangements when in contact with the H1F6H*n*SH surfaces, but the H-bonding network is still strong enough to interrupt a full reorientation of the interfacial molecules when in contact with HC−FC dipoles of the H1F6H*n*SH FSAMs. However, in the case of cyclohexanol, which possesses a bulky cyclohexane ring and only one OH group, the H-bonding network within the liquid appears to be too weak to overcome the dipole−dipole interactions between the liquid and the surface of the H1F6H*n*SH FSAMs, leading to an inversion of the odd−even trend exhibited by glycerol. Unfortunately, the last of the test contacting liquids chosen for this series, isopropanol, is a relatively small molecule with a low surface tension; consequently, the advancing contact angles measured on our FSAMs using this probe liquid were quite low (on the order of perfluorodecalin), hindering our ability to interpret fully the results obtained.

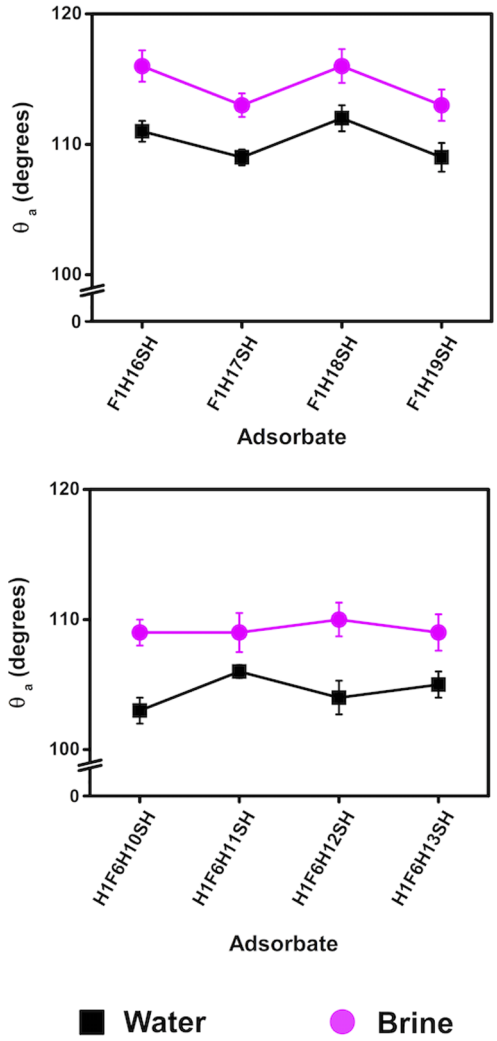


**Figure 8.** Wettability data of brine and water on the F1H*n*SH (upper plot) and H1F6H*n*SH (lower plot) FSAMs on gold. Lines connecting the data points are simply guides for the eye. Error bars that are not visible fall within the symbols.

*Formamide and Its Analogues.* Figure 10 shows the contact angles of FA, MFA, and DMF—a series of probe liquids with decreasing H-bonding sites via the progressive substitution of a proton with a methyl substituent on the amide nitrogen. These contacting liquids provide a straightforward comparison of the effect that the availability of H-bonding sites has on the contact angle trends for the SAMs derived from F1H*m*SH and H1F6H*n*SH. Formamide, in contact with the H1F6H*n*SH films, exhibits an odd−even trend opposite to that observed for this contacting liquid on the F1H*m*SH films. As with the other protic liquids discussed above, we attribute this inverse odd−even effect to the existence of a strong hydrogen-bonding


DOI: 10.1021/acs.chemmater.5b03411
*Chem. Mater.* 2015, 27, 7433−7446

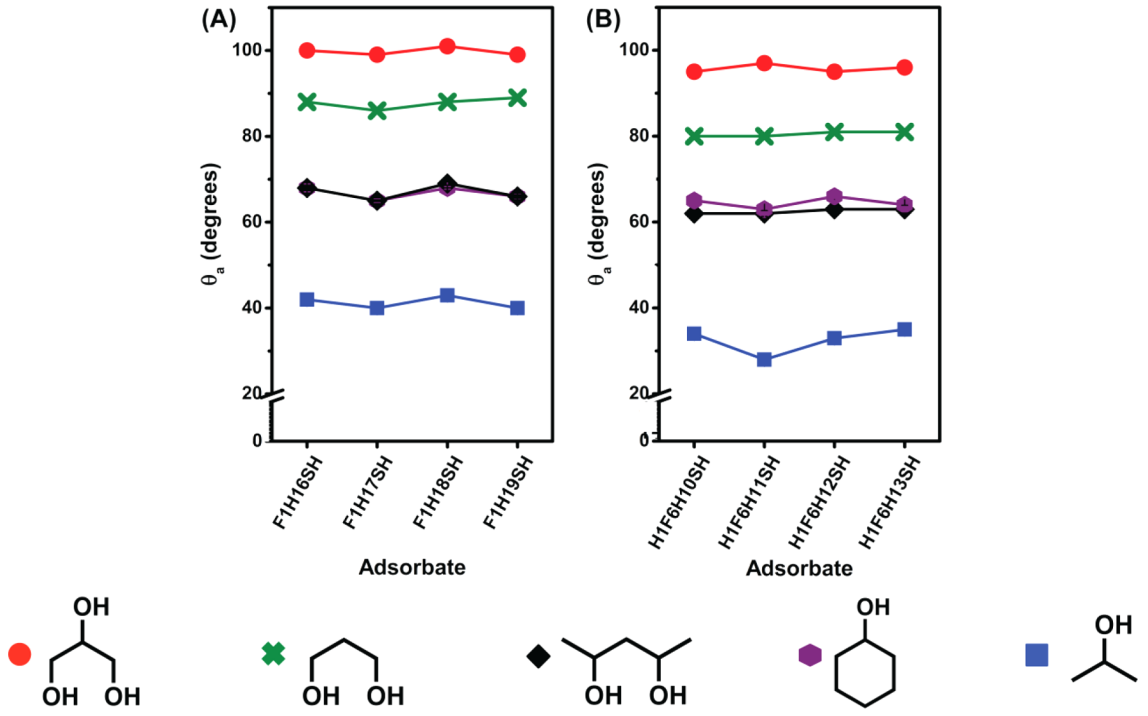


**Figure 9.** Wettability data of glycerol, 1,3-propanediol, 2,4-pentanediol, cyclohexanol, and isopropanol on SAMs derived from the adsorption of (A) F1H*m*SH and (B) H1F6H*n*SH on gold. Lines connecting the data points are simply guides for the eye. Error bars that are not visible fall within the symbols.

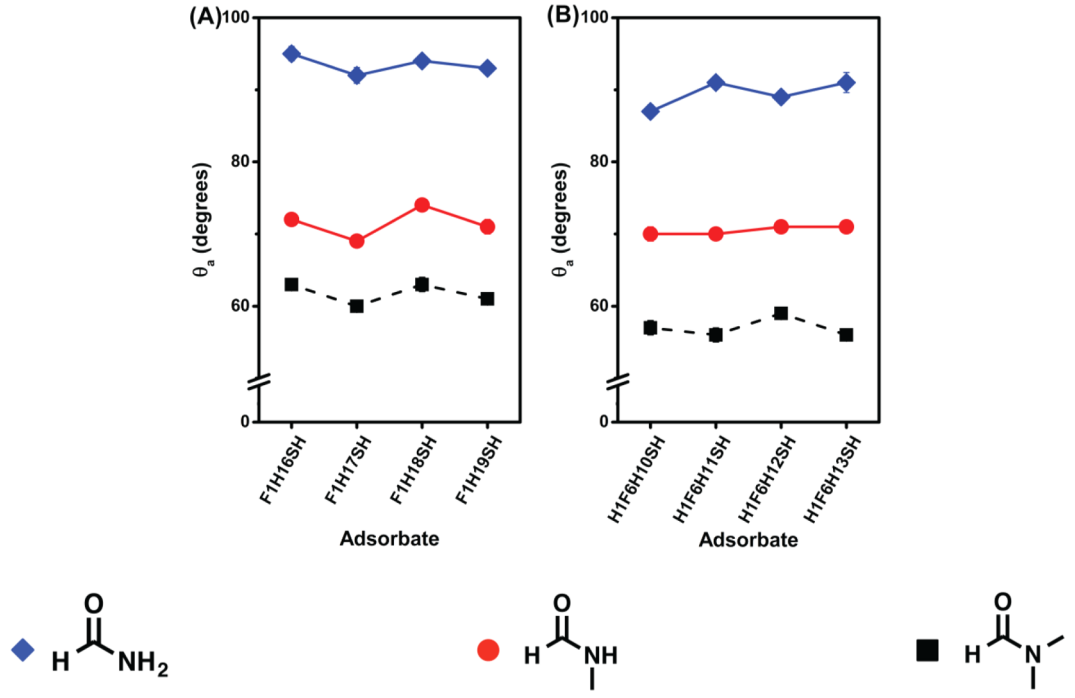


**Figure 10.** Wettability data of FA, MFA, and DMF on SAMs derived from the adsorption of (A) F1H*m*SH and (B) H1F6H*n*SH on gold. Lines connecting the data points are simply guides for the eye. Error bars that are not visible fall within the symbols.

network in the contacting liquid, which gives rise to unfavorable interfacial interactions between the dipoles of the protic liquid ($\delta^+$) and that of the HC−FC dipoles ($\delta^+$) of the chain termini of the H1F6H*n*SH FSAMs. However, with the substitution of one methyl group for an amide proton to give methylformamide (MFA, $\gamma_{LV}$ = 37.96 mN/m), the resulting contact angle data reveal that the H-bonding network within the interfacial region of this contacting liquid is sufficiently disrupted to reduce this interaction and consequently eliminate the odd−even trend on the H1F6H*n*SH films. Furthermore, with the substitution of the second methyl group for the remaining amide proton to give dimethylformamide (DMF, $\gamma_{LV}$ = 34.4 mN/m), the resulting contact angle data show an odd−even trend on the H1F6H*n*SH FSAMs opposite to that observed for



DOI: 10.1021/acs.chemmater.5b03411
*Chem. Mater.* 2015, 27, 7433−7446

formamide. In contrast, we note that all three of these contacting liquids (in fact, all of the polar liquids examined here) give rise to a consistent odd−even trend on the F1H*m*SH or "$CF_3$-terminated" films.

As a whole, the studies involving water, brine, glycerol, formamide, and the analogues of the latter two contacting liquids support a model in which highly hydrogen-bonded liquid molecules at the liquid−FSAM interface resist the adoption of a more favorable interfacial orientation (on the basis of polarity) when in the presence of the inverted HC−FC dipole. Given that strongly hydrogen-bonded liquids possess high surface tension, it is interesting to note that the effect of the HC−FC dipoles on the polar contacting liquids appears to correlate with the magnitude of their surface tension; that is, polar liquids with relatively high surface tension follow an odd−even trend opposite to that observed for polar liquids with relatively low surface tension (see Figures 8−10). More broadly, the collective results presented demonstrate that the unusual and rich wettability behavior observed on the new H1F6H*n*SH films arises from their unique structure and the orientation of their molecular dipole.

## CONCLUSIONS

We prepared a series of new $CH_3$-capped, partially fluorinated alkanethiols (H1F6H*n*SH) and used them to generate FSAMs that expose an array of inverted surface dipoles on gold surfaces. Upon developing the SAMs in ethanol for 48 h, followed by further equilibration at 40 °C for 24 h, formation of monolayer films was confirmed by both ellipsometry and XPS. When compared to normal alkanethiolate SAMs (H*x*SH), XPS analysis of the C 1s binding energies indicated that the packing density of the H1F6H*n*SH FSAMs was less than that of the H*x*SH SAMs. Nonetheless, the alkyl spacers of the H1F6H*n*SH FSAMs adopted highly ordered, *trans*-extended conformations, as indicated by the antisymmetric C−H stretching vibrations of the methylene units in the PM-IRRAS spectra. Therefore, we concluded that the observed shifts in the C 1s binding energies in the XPS spectra probably arise from the increased vdW diameter of the fluorinated helix, leading to an increased interchain distance.

Wettability studies allowed us to examine systematically the effect of the inverted dipoles (HC−FC) on the interfacial energies. Contact angle values of nonpolar (dispersive) contacting liquids showed that the H1F6H*n*SH FSAMs have an oleophobic character greater than or equal to that of the H*x*SH SAMs, suggesting that the underlying fluorocarbon units might be partially exposed at the interface. Further, wettability studies using polar contacting liquids revealed that the H1F6H*n*SH FSAMs are more wettable than their hydrocarbon and $CF_3$-terminated counterparts. We attribute the enhanced wettability to the presence of the interfacial HC−FC dipole at the termini of the new adsorbates. In addition, the larger diameter of the fluorinated layer underneath the terminal methyl unit allows for the polar molecules to intercalate into the interfacial region of the H1F6H*n*SH films more than the F1H*m*SH films. We also observed odd−even wettability effects for both nonpolar and polar liquids on the H1F6H*n*SH films, allowing us to draw several conclusions regarding the effect of the HC−FC surface dipoles on the interfacial properties versus that of the influence of the underlying perfluorinated segment: (1) for nonpolar liquids on the H1F6H*n*SH films, the systematic variation in exposure of the underlying perfluorinated segment to the liquid−SAM interface renders the *even* monolayers more wettable than the *odd* ones; (2) for polar aprotic liquids, systematic variation in the orientation of the surface dipole generated from the HC−FC junction in the H1F6H*n*SH films leads the surface dipole to be largely uncompensated in the *even* H1F6H*n*SH monolayers as compared to the *odd* ones, yielding an increase in the dipole−dipole interactions between the contacting liquid and the *even* FSAMs (more wettable) as compared to the *odd* FSAMs (less wettable); (3) for polar protic liquids, the observed odd−even effects on the H1F6H*n*SH films were sometimes analogous and sometimes opposite to that of the corresponding $CF_3$-terminated films due to a combination of dipole−dipole interactions and H-bonding within the contacting liquids that restricted the molecular organization/reorientation of the liquid molecules within the interfacial region of the liquid drop in response to the dipoles at the liquid−SAM interface, thus separating the effect of the polarity of the surface dipole (i.e., HC−FC vs FC−HC) from its interfacial orientation. Nevertheless, the compelling story from the wetting behavior of contacting liquids on the FSAMs derived from both F1H*m*SH and H1F6H*n*SH is that interactions at the liquid−SAM interface are governed by a variety of factors that arise from the surface-confined dipoles interacting with the interfacial molecules of a contacting liquid, giving rise to both dipole−dipole interactions (i.e., Keesom forces for polar contacting liquids) and dipole−induced dipole interactions (i.e., Debye forces for nonpolar contacting liquids).

As a whole, these studies on fluorocarbon films open new avenues for controlling the properties of 2D macro-systems similar to what has been observed on other dipole-bearing SAM systems, such as work function and friction as outlined in a recent review article.[6,63,64] Therefore, subsequent work will include investigations of the surface orientation of the methyl terminal group in the H1F6H*n*SH FSAMs using a more interface-sensitive spectroscopic technique (i.e., sum frequency generation spectroscopy, SFG) along with investigations utilizing isotopic labeling. In addition, the magnitude and direction of the molecular dipole need to be determined experimentally, possibly by UV-photoelectron spectroscopy (UPS), and compared to the results described herein. Finally, the effect of this new type of surface dipole (HC−FC) on the frictional properties of these films will also be explored, recognizing that having a small alkyl tailgroup placed on a wider rigid perfluorinated segment might reduce the interfacial friction of these model boundary lubricants.

## ASSOCIATED CONTENT

### Supporting Information

The Supporting Information is available free of charge on the ACS Publications website at DOI: 10.1021/acs.chemmater.5b03411.

Detailed information regarding the materials and synthetic procedures for preparing the H1F6H*n*SH and F1H*m*SH adsorbates, including $^1$H, $^{19}$F, and $^{13}$C NMR spectra for the final compounds (Figures S1−S20); instrumental procedures used to conduct this research, detailed contact angle data, additional XPS data and analysis, supplementary PM-IRRAS data and analysis, and background information for the molecular models prepared for this report (PDF)



DOI: 10.1021/acs.chemmater.5b03411
*Chem. Mater.* 2015, 27, 7433−7446

## AUTHOR INFORMATION


### Corresponding Author

*E-mail: trlee@uh.edu.


### Notes

The authors declare no competing financial interest.

## ACKNOWLEDGMENTS

We are grateful for generous financial support from the National Science Foundation (CHE-1411265), the Robert A. Welch Foundation (E-1320), and the Texas Center for Superconductivity at the University of Houston.

## REFERENCES


(1) Gentilini, C.; Boccalon, M.; Pasquato, L. Straightforward Synthesis of Fluorinated Amphiphilic Thiols. *Eur. J. Org. Chem.* **2008**, *2008*, 3308−3313.

(2) Gentilini, C.; Evangelista, F.; Rudolf, P.; Franchi, P.; Lucarini, M.; Pasquato, L. Water-Soluble Gold Nanoparticles Protected by Fluorinated Amphiphilic Thiolates. *J. Am. Chem. Soc.* **2008**, *130*, 15678−15682.

(3) Lee, S.; Park, J.-S.; Lee, T. R. The Wettability of Fluoropolymer Surfaces: Influence of Surface Dipoles. *Langmuir* **2008**, *24*, 4817−4826.

(4) Chen, T.-H.; Popov, I.; Zenasni, O.; Daugulis, O.; Miljanic, O. S. Superhydrophobic perfluorinated metal-organic frameworks. *Chem. Commun.* **2013**, *49*, 6846−6848.

(5) Santos, C. M.; Kumar, A.; Zhang, W.; Cai, C. Functionalization of fluorous thin films via "click" chemistry. *Chem. Commun.* **2009**, 2854−2856.

(6) Zenasni, O.; Jamison, A. C.; Lee, T. R. The impact of fluorination on the structure and properties of self-assembled monolayer films. *Soft Matter* **2013**, *9*, 6356−6370.

(7) Barriet, D.; Lee, T. R. Fluorinated self-assembled monolayers: composition, structure and interfacial properties. *Curr. Opin. Colloid Interface Sci.* **2003**, *8*, 236−242.

(8) O'Hagan, D. Understanding organofluorine chemistry. An introduction to the C-F bond. *Chem. Soc. Rev.* **2008**, *37*, 308−319.

(9) Bunn, C. W.; Howells, E. R. Structures of Molecules and Crystals of Fluoro-Carbons. *Nature* **1954**, *174*, 549−551.

(10) Clark, E. S. The molecular conformations of polytetrafluoroethylene: forms II and IV. *Polymer* **1999**, *40*, 4659−4665.

(11) Golden, W. G.; Brown, E. M.; Solem, S. E.; Zoellner, R. W. Complete conformational analyses of perfluoro-n-pentane, perfluoro-n-hexane, and perfluoro-n-heptane. *J. Mol. Struct.: THEOCHEM* **2008**, *867*, 22−27.

(12) Krafft, M. P.; Riess, J. G. Chemistry, Physical Chemistry, and Uses of Molecular Fluorocarbon−Hydrocarbon Diblocks, Triblocks, and Related Compounds—Unique "Apolar" Components for Self-Assembled Colloid and Interface Engineering. *Chem. Rev.* **2009**, *109*, 1714−1792.

(13) Graupe, M.; Takenaga, M.; Koini, T.; Colorado, R., Jr.; Lee, T. R. Oriented Surface Dipoles Strongly Influence Interfacial Wettabilities. *J. Am. Chem. Soc.* **1999**, *121*, 3222−3223.

(14) Graupe, M.; Koini, T.; Wang, V. Y.; Nassif, G. M.; Colorado, R., Jr; Villazana, R. J.; Dong, H.; Miura, Y. F.; Shmakova, O. E.; Lee, T. R. Terminally perfluorinated long-chain alkanethiols. *J. Fluorine Chem.* **1999**, *93*, 107−115.

(15) Kim, H. I.; Koini, T.; Lee, T. R.; Perry, S. S. Systematic Studies of the Frictional Properties of Fluorinated Monolayers with Atomic Force Microscopy: Comparison of CF3- and CH3-Terminated Films. *Langmuir* **1997**, *13*, 7192−7196.

(16) Kim, H. I.; Graupe, M.; Oloba, O.; Koini, T.; Imaduddin, S.; Lee, T. R.; Perry, S. S. Molecularly Specific Studies of the Frictional Properties of Monolayer Films: A Systematic Comparison of CF3-, (CH3)2CH-, and CH3-Terminated Films. *Langmuir* **1999**, *15*, 3179−3185.

(17) Pflaum, J.; Bracco, G.; Schreiber, F.; Colorado, R., Jr; Shmakova, O. E.; Lee, T. R.; Scoles, G.; Kahn, A. Structure and electronic properties of CH3- and CF3-terminated alkanethiol monolayers on Au(1 1 1): a scanning tunneling microscopy, surface X-ray and helium scattering study. *Surf. Sci.* **2002**, *498*, 89−104.

(18) Colorado, R. J.; Graupe, M.; Kim, H. I.; Takenaga, M.; Oloba, O.; Lee, S.; Perry, S. S.; Lee, T. R. Interfacial Properties of Specifically Fluorinated Self-Assembled Monolayer Films. *ACS Symp. Ser.* **2001**, *781*, 58−75.

(19) Colorado, R., Jr.; Lee, T. R. Physical organic probes of interfacial wettability reveal the importance of surface dipole effects. *J. Phys. Org. Chem.* **2000**, *13*, 796−807.

(20) Colorado, R., Jr.; Lee, T. R. Wettabilities of Self-Assembled Monolayers on Gold Generated from Progressively Fluorinated Alkanethiols. *Langmuir* **2003**, *19*, 3288−3296.

(21) Schönherr, H.; Vancso, G. J. AFM Study on Lattice Orientation and Tribology of SAMS of Fluorinated Thiols and Disulfides on Au(111): The Influence of the Molecular Structure. *ACS Symp. Ser.* **2001**, *787*, 15−30.

(22) Pujari, S. P.; Scheres, L.; Weidner, T.; Baio, J. E.; Cohen Stuart, M. A.; van Rijn, C. J. M.; Zuilhof, H. Covalently Attached Organic Monolayers onto Silicon Carbide from 1-Alkynes: Molecular Structure and Tribological Properties. *Langmuir* **2013**, *29*, 4019−4031.

(23) Pujari, S. P.; Spruijt, E.; Cohen Stuart, M. A.; van Rijn, C. J. M.; Paulusse, J. M. J.; Zuilhof, H. Ultralow Adhesion and Friction of Fluoro-Hydro Alkyne-Derived Self-Assembled Monolayers on H-Terminated Si(111). *Langmuir* **2012**, *28*, 17690−17700.

(24) Li, S.; Cao, P.; Colorado, R., Jr.; Yan, X.; Wenzl, I.; Shmakova, O. E.; Graupe, M.; Lee, T. R.; Perry, S. S. Local Packing Environment Strongly Influences the Frictional Properties of Mixed CH3- and CF3-Terminated Alkanethiol SAMs on Au(111). *Langmuir* **2005**, *21*, 933−936.

(25) In a review article, we found one mention of a solitary film generated from $CH_3(CF_2)_{11}CO_2H$ on an undefined substrate: Johnson, R., Jr.; Dettre, R. H. Wetting of Low-Energy Surfaces. *Surf. Sci. Series* **1993**, *49*, 1. However, the absence of any primary data and the lack of any characterization data for the adsorbate, coupled with the fact that the authors reported wettability data for only one contacting liquid (and that liquid, HD, gave a higher contact angle value than we observed on any of our H1F6H*n*SH films), lead us to question the purity/quality of the films and the adequacy of the report as a whole.

(26) Chinwangso, P. Self-assembled monolayers generated from custom-tailored spiroalkanedithiols offer unprecedented multi-component interfaces. Ph.D. Thesis, University of Houston, Houston, TX, 2009.

(27) Bain, C. D.; Troughton, E. B.; Tao, Y. T.; Evall, J.; Whitesides, G. M.; Nuzzo, R. G. Formation of monolayer films by the spontaneous assembly of organic thiols from solution onto gold. *J. Am. Chem. Soc.* **1989**, *111*, 321−335.

(28) Barriet, D. Synthesis and characterization of specifically fluorinated and structurally tailored self-assembled monolayers on gold. Ph.D. Thesis, University of Houston, Houston, TX, 2005.

(29) Colorado, R., Jr.; Lee, T. R. Attenuation Lengths of Photoelectrons in Fluorocarbon Films. *J. Phys. Chem. B* **2003**, *107*, 10216−10220.

(30) Garg, N.; Lee, T. R. Self-Assembled Monolayers Based on Chelating Aromatic Dithiols on Gold. *Langmuir* **1998**, *14*, 3815−3819.

(31) Colorado, R., Jr.; Graupe, M.; Shmakova, O. E.; Villazana, R. J.; Lee, T. R. Structural Properties of Self-Assembled Monolayers on Gold Generated from Terminally Fluorinated Alkanethiols. *ACS Symp. Ser.* **2001**, *781*, 276−292.

(32) Yuan, Y.; Yam, C. M.; Shmakova, O. E.; Colorado, R., Jr.; Graupe, M.; Fukushima, H.; Moore, H. J.; Lee, T. R. Solution-Phase Desorption of Self-Assembled Monolayers on Gold Derived From Terminally Perfluorinated Alkanethiols. *J. Phys. Chem. C* **2011**, *115*, 19749−19760.

(33) Frey, S.; Heister, K.; Zharnikov, M.; Grunze, M.; Tamada, K.; Colorado, R., Jr.; Graupe, M.; Shmakova, O. E.; Lee, T. R. Structure of




DOI: 10.1021/acs.chemmater.5b03411
*Chem. Mater.* 2015, 27, 7433−7446

self-assembled monolayers of semifluorinated alkanethiols on gold and silver substrates. *Isr. J. Chem.* **2000**, *40*, 81−97.
(34) Alves, C. A.; Porter, M. D. Atomic force microscopic characterization of a fluorinated alkanethiolate monolayer at gold and correlations to electrochemical and infrared reflection spectroscopic structural descriptions. *Langmuir* **1993**, *9*, 3507−3512.
(35) Tamada, K.; Ishida, T.; Knoll, W.; Fukushima, H.; Colorado, R., Jr.; Graupe, M.; Shmakova, O. E.; Lee, T. R. Molecular Packing of Semifluorinated Alkanethiol Self-Assembled Monolayers on Gold: Influence of Alkyl Spacer Length. *Langmuir* **2001**, *17*, 1913−1921.
(36) Zenasni, O.; Jamison, A. C.; Marquez, M. D.; Lee, T. R. Self-assembled monolayers on gold generated from terminally perfluorinated alkanethiols bearing propyl vs. ethyl hydrocarbon spacers. *J. Fluorine Chem.* **2014**, *168*, 128−136.
(37) Laibinis, P. E.; Whitesides, G. M.; Allara, D. L.; Tao, Y. T.; Parikh, A. N.; Nuzzo, R. G. Comparison of the structures and wetting properties of self-assembled monolayers of n-alkanethiols on the coinage metal surfaces, copper, silver, and gold. *J. Am. Chem. Soc.* **1991**, *113*, 7152−7167.
(38) Castner, D. G.; Hinds, K.; Grainger, D. W. X-ray Photoelectron Spectroscopy Sulfur 2p Study of Organic Thiol and Disulfide Binding Interactions with Gold Surfaces. *Langmuir* **1996**, *12*, 5083−5086.
(39) Rittikulsittichai, S.; Jamison, A. C.; Lee, T. R. Self-Assembled Monolayers Derived from Alkoxyphenylethanethiols Having One, Two, and Three Pendant Chains. *Langmuir* **2011**, *27*, 9920−9927.
(40) Ishida, T.; Hara, M.; Kojima, I.; Tsuneda, S.; Nishida, N.; Sasabe, H.; Knoll, W. High Resolution X-ray Photoelectron Spectroscopy Measurements of Octadecanethiol Self-Assembled Monolayers on Au(111). *Langmuir* **1998**, *14*, 2092−2096.
(41) Ishida, T.; Nishida, N.; Tsuneda, S.; Hara, M.; Sasabe, H.; Knoll, W. Alkyl Chain Length Effect on Growth Kinetics of n-Alkanethiol Self-Assembled Monolayers on Gold Studied by X-Ray Photoelectron Spectroscopy. *Jpn. J. Appl. Phys.* **1996**, *35*, L1710−L1713.
(42) Porter, M. D.; Bright, T. B.; Allara, D. L.; Chidsey, C. E. D. Spontaneously organized molecular assemblies. 4. Structural characterization of n-alkyl thiol monolayers on gold by optical ellipsometry, infrared spectroscopy, and electrochemistry. *J. Am. Chem. Soc.* **1987**, *109*, 3559−3568.
(43) Snyder, R. G.; Strauss, H. L.; Elliger, C. A. Carbon-hydrogen stretching modes and the structure of n-alkyl chains. 1. Long, disordered chains. *J. Phys. Chem.* **1982**, *86*, 5145−5150.
(44) MacPhail, R. A.; Strauss, H. L.; Snyder, R. G.; Elliger, C. A. Carbon-hydrogen stretching modes and the structure of n-alkyl chains. 2. Long, all-trans chains. *J. Phys. Chem.* **1984**, *88*, 334−341.
(45) Fukushima, H.; Seki, S.; Nishikawa, T.; Takiguchi, H.; Tamada, K.; Abe, K.; Colorado, R., Jr.; Graupe, M.; Shmakova, O. E.; Lee, T. R. Microstructure, Wettability, and Thermal Stability of Semifluorinated Self-Assembled Monolayers (SAMs) on Gold. *J. Phys. Chem. B* **2000**, *104*, 7417−7423.
(46) Durig, J. R.; Yu, Z.; Guirgis, G. A. Conformational stability, barriers to internal rotation, vibrational assignment, and ab initio calculations of 2,2-difluorobutane. *J. Mol. Struct.* **1999**, *509*, 115−135.
(47) Dalvi, V. H.; Rossky, P. J. Molecular origins of fluorocarbon hydrophobicity. *Proc. Natl. Acad. Sci. U. S. A.* **2010**, *107*, 13603−13607.
(48) Smallwood, I. M. *Handbook of Organic Solvent Properties*; John Wiley & Sons: New York, 1996.
(49) Yaws, C. L. *Chemical properties handbook: Physical, thermodynamic, environmental, transport, safety, and health related properties for organic and inorganic chemicals*; McGraw-Hill: New York, 1999.
(50) Fowkes, F. M.; Riddle, F. L., Jr; Pastore, W. E.; Weber, A. A. Interfacial interactions between self-associated polar liquids and squalane used to test equations for solid—liquid interfacial interactions. *Colloids Surf.* **1990**, *43*, 367−387.
(51) Jańczuk, B.; Białłopiotrowicz, T. Surface free-energy components of liquids and low energy solids and contact angles. *J. Colloid Interface Sci.* **1989**, *127*, 189−204.
(52) Baghbanzadeh, M.; Simeone, F. C.; Bowers, C. M.; Liao, K.-C.; Thuo, M.; Baghbanzadeh, M.; Miller, M. S.; Carmichael, T. B.; Whitesides, G. M. Odd−Even Effects in Charge Transport across n-Alkanethiolate-Based SAMs. *J. Am. Chem. Soc.* **2014**, *136*, 16919−16925.
(53) Barriet, D.; Chinwangso, P.; Lee, T. R. Can Cyclopropyl-Terminated Self-Assembled Monolayers on Gold Be Used to Mimic the Surface of Polyethylene? *ACS Appl. Mater. Interfaces* **2010**, *2*, 1254−1265.
(54) Graupe, M.; Koini, T.; Kim, H. I.; Garg, N.; Miura, Y. F.; Takenaga, M.; Perry, S. S.; Lee, T. R. Wettability and friction of CF3-terminated monolayer films on gold. *Mater. Res. Bull.* **1999**, *34*, 447−453.
(55) Nelson, R. D.; Lide, D. R.; Maryott, A. A. Selected values of electric dipole moments for molecules in the gas phase. *Natl. Stand. Ref. Data Ser.: Natl. Bur. Stand. 10*, **1967**.
(56) Riddick, J. A.; Bunger, W. B.; Sakano, T. K. *Organic Solvents*, Fourth ed.; John Wiley & Sons: New York, 1986.
(57) Petrov, J. G.; Andreeva, T. D.; Möhwald, H. Fluorination of the Hydrophilic Head Accelerates the Collapse of the Monolayer but Stabilizes the Bilayer of a Long-Chain Trifluoroethyl Ether on Water. *Langmuir* **2006**, *22*, 4136−4143.
(58) Du, Q.; Freysz, E.; Shen, Y. R. Surface vibrational spectroscopic studies of hydrogen bonding and hydrophobicity. *Science* **1994**, *264*, 826.
(59) Du, Q.; Superfine, R.; Freysz, E.; Shen, Y. R. Vibrational spectroscopy of water at the vapor/water interface. *Phys. Rev. Lett.* **1993**, *70*, 2313−2316.
(60) Shen, Y. R.; Ostroverkhov, V. Sum-Frequency Vibrational Spectroscopy on Water Interfaces: Polar Orientation of Water Molecules at Interfaces. *Chem. Rev.* **2006**, *106*, 1140−1154.
(61) Scatena, L. F.; Brown, M. G.; Richmond, G. L. Water at Hydrophobic Surfaces: Weak Hydrogen Bonding and Strong Orientation Effects. *Science* **2001**, *292*, 908−912.
(62) Raymond, E. A.; Richmond, G. L. Probing the Molecular Structure and Bonding of the Surface of Aqueous Salt Solutions. *J. Phys. Chem. B* **2004**, *108*, 5051−5059.
(63) Hohman, J. N.; Zhang, P.; Morin, E. I.; Han, P.; Kim, M.; Kurland, A. R.; McClanahan, P. D.; Balema, V. P.; Weiss, P. S. Self-Assembly of Carboranethiol Isomers on Au{111}: Intermolecular Interactions Determined by Molecular Dipole Orientations. *ACS Nano* **2009**, *3*, 527−536.
(64) Abu-Husein, T.; Schuster, S.; Egger, D. A.; Kind, M.; Santowski, T.; Wiesner, A.; Chiechi, R.; Zojer, E.; Terfort, A.; Zharnikov, M. The Effects of Embedded Dipoles in Aromatic Self-Assembled Monolayers. *Adv. Funct. Mater.* **2015**, *25*, 3943−3957.


DOI: 10.1021/acs.chemmater.5b03411
*Chem. Mater.* 2015, 27, 7433−7446